Journal of Applied Polymer Science

Influence of the polymorphism of cellulose on the formation of nanocrystals and their application in chitosan/nanocellulose composites

Sławomir Borysiak, Aleksandra Grząbka-Zasadzińska
Institute of Chemical Technology and Engineering, Poznań University of Technology, Berdychowo 4, Poland
Correspondence to: S. Borysiak (E-mail: slawomir.borysiak@put.poznan.pl)

ABSTRACT: In this study, we evaluated the physicochemical properties of the chitosan/nanocellulose composites. Wide-angle X-ray scattering was applied to define the supermolecular structure of the materials, the laser diffracting technique was used to characterize the particle sizes, and scanning electron microscopy was used to evaluate the morphologies of the samples. The tensile properties of the composite films were also determined. Cellulose pulp was mercerized with 16% sodium hydroxide to give only cellulose II. Cellulose I and cellulose II were subsequently hydrolyzed with 64% sulfuric acid. As a result, nanocellulose I (NCC I) from cellulose I and nanocellulose II (NCC II) from cellulose II were produced. The mercerization of cellulose pulp contributed to a significant particle size reduction; more than 50% of the particles of the NCC II sample and only 36% of the particles of the NCC I sample were smaller than 100 nm. Chitosan composite films containing 5, 10, and 20% w/w of nanocelluloses were prepared by a solvent casting method. This was the first study investigating the influence of the crystallographic forms of cellulose on the formation of nanocrystals. © 2015 Wiley Periodicals, Inc. J. Appl. Polym. Sci. **2016**, *133*, 42864.

KEYWORDS: composites; films; mechanical properties; nanoparticles; nanowires and nanocrystals

Received 23 October 2014; accepted 22 August 2015
DOI: 10.1002/app.42864

INTRODUCTION

The vigorous growth of the biocomposites market has been caused mainly by increasing ecological awareness. Limiting the influence of industry on the environment and the very fast growing market of plastics along with the significant shortage of landfill space are the main reasons for the contribution of the development of new types of biocomposites.[1,2]

Cellulose, a linear polymer of D-anhydroglucopyranose units linked together by β-1,4-glucosidic bonds, occurs in wood, cotton, hemp, flax, and other plant-based materials.[3] Currently, very much attention has been paid to it; one of the reasons for that state of affairs is its high availability and low price. Cellulose can be transformed into nanocellulose, a very promising composite nanofiller that combines biodegradability and distinctive properties. There are three subcategories of nanocellulose: microfibrilated cellulose, nanocrystalline cellulose (NCC), and bacterial nanocellulose.[4] NCC (known also as *whiskers*) is formed by rigid rodlike particles whose length varies from 100 nm to several micrometers and whose width ranges from 5 to 70 nm. Such particles can be successfully applied as reinforcements in nanocomposites to improve their barrier and mechanical properties. There are few challenges with NCC; the most significant one is probably the efficient production of NCC with an established size, aspect ratio, and controlled surface.[5]

Chitosan, a polysaccharide of marine origin, is also enthusiastically used for the formation of composites. It is produced from chitin by partial alkaline *N*-deacetylation, and it consists of *N*-acetyl glucosamine and D-glucosamine units linked together with 1,4-β linkages. The presence of reactive amino and hydroxyl groups in the chitosan structure enables chemical modifications, but is also responsible for its poor solubility in organic solvents.[5,6] Chitosan films have one major drawback: they are brittle and thus need a plasticizer that increases their flexibility and mechanical properties.[7,8]

Both nanometric cellulose and chitosan are polysaccharides that due to their chemical compatibility, can be combined without any extra modifications. Moreover, this combination is a green process that can be conducted in aqueous media. The resulting composite combines the physicochemical properties of chitosan and the remarkable mechanical properties of nanocellulose. The addition of nanocellulose particles to polymeric matrices has shown that materials with a high transparency and exceptional thermal, mechanical, and barrier properties can be obtained.[9,10]

Khan *et al.*[11] proved that only 5% NCC incorporated into the chitin matrix decreased the water vapor permeability by 27%. Other researchers[12] showed that the water solubility of chitosan/nanocellulose films relied on the concentrations of NCC and glycerol. It was also possible to prepare chitosan/nanocellulose films with transparency in the range from 85 to 92%. Azaredo *et al.*[8] produced a nanocomposite film with 15% cellulose nanofibers and plasticized with 18% glycerol that in terms of strength and stiffness, turned out to be comparable to some synthetic polymers. Chitosan/nanocellulose composites with the addition of glycerol were also investigated as films for extending the shelf life of ground meat.[13] Velásquez-Cock *et al.*[14] studied the influence of the acid type in the production of chitosan films reinforced with bacterial nanocellulose. The mechanical properties of these films were more influenced by acetic acid (CH_3COOH) than by lactic acid. Samples prepared from CH_3COOH showed higher Young's modulus (YM) and tensile strength (TS) values compared to those prepared with lactic acid (e.g., 12.3 and 3.3 MPa for CH_3COOH and lactic acid, respectively), even though the same concentrations of reinforcement were maintained.

It is well known that nanoscaled filler, because of its high surface area, can effectively improve the mechanical properties of the polymer matrix. However, in terms of nanocellulose composites, the production of an efficient compounding of nanocellulose with the polymer matrix is related to the surface modification of nanocellulose, which limits the aggregation of hydrophilic cellulose nanocrystals. Another interesting issue that affects the compounding properties of nanocellulose-based composites is the polymorphism of cellulose. The crystal structure of native cellulose I can be converted to cellulose II with sodium hydroxide (NaOH), a treatment known as mercerization.[3] After this process, the original parallel-chain crystal structure of cellulose I is converted to antiparallel chains of cellulose II.[15] In cellulose II, hydrogen bonds connect all of the neighboring cellulose molecules, whereas in cellulose I, van der Waals forces are responsible for its sheet structure.[16–18] The dissimilarity of cellulose II exerts a beneficial effect on the physicochemical properties. According to the literature,[19–21] mercerization of the cellulose filler leads to changes in the nucleation abilities. The high nucleation activity of only one polymorphic variety of cellulose can be a consequence of the match between the crystallographic structures of cellulose and the polymer matrix, as studied in detail by Quillin *et al.*[22]

To the best of our knowledge, the role of the polymorph structures of nanosized cellulose and their application in composites has not yet been reported. As follows from the survey of literature in the field, most of the research work on cellulose has been concerned only with the influence of polymorphic cellulose on the final properties of composite materials. An analysis of the literature indicated that the polymorphic structure of cellulose may influence the formation of nanosized cellulose and the determination of the particle size distribution, and therefore, taking this issue into account is justified. The aim of this study was to evaluate the effect of the crystallographic form of cellulose on nanocellulose formation and its influence on the properties of composites, as this has not been studied so far.

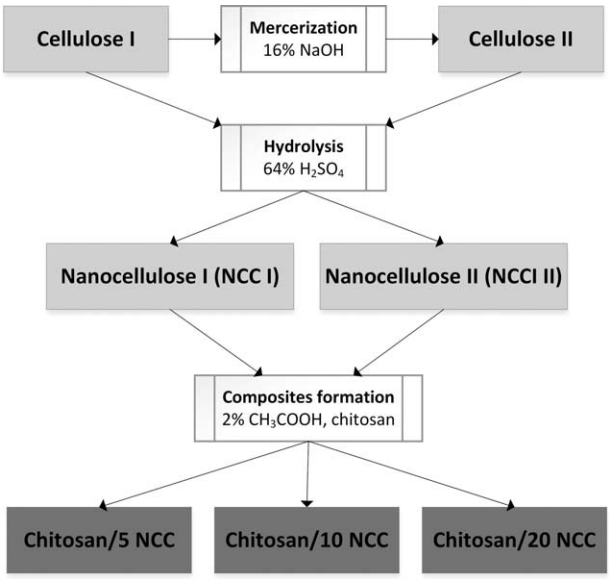

Figure 1. Flowchart of the composite preparation.

The knowledge of this subject is essential for the design production of celluloses that will be appropriate for the production of a great number of particles with nanometric size. In this research, chitosan/nanocellulose film composites were prepared, and their physicochemical properties, including their mechanical properties and supermolecular structure, were evaluated.

EXPERIMENTAL

Raw Materials

Cellulose pulp, with particles sizes in the range from 2 to 20 μm and average degrees of polymerization from 400 to 500, was supplied by Macherey-Nagel. Chitosan, with molecular weights from 100.000 to 300.000 and a water content below 10%, was purchased from Acros Organics. Pure NaOH (Chempur) was used for the preparation of a 16% solution and was subsequently used as a mercerizing agent. Sulfuric acid (H_2SO_4; 95%, POCH S.A.) was diluted to obtain a 64% solution, which was used as the hydrolytic agent during nanocellulose preparation. CH_3COOH (80%, POCH S.A.) was diluted to a 2% solution and used for composite formation. Figure 1 shows a flowchart of the composite preparation.

Cellulose Pulp Mercerization

An amount of 15 g of cellulose pulp was treated with 150 mL of an aqueous solution of NaOH (16%) at room temperature. After 5 min of continuous stirring, 150 mL of water was added to stop the mercerization process. The suspension was centrifuged at 10,000 rpm for 10 min. Afterward, the pulp was washed 10 times with distilled water to remove the excess NaOH and then dried in air at gradually increasing temperatures from 70 to 95°C.

Nanocellulose I (NCC I) Preparation

NCC I was obtained through the controlled hydrolysis of cellulose. An amount of 10 g of cellulose I was immersed in 100 mL of 64% H_2SO_4 and continuously stirred. After a temperature of 45°C was reached, the reaction was continued for the next 30

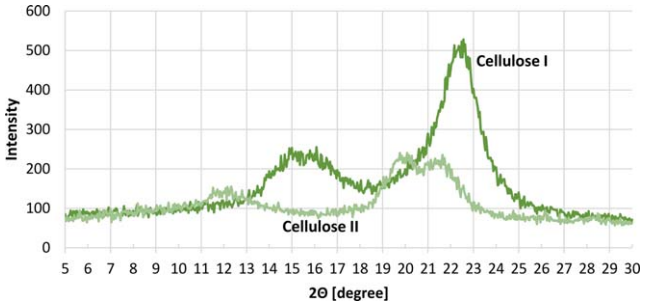

Figure 2. WAXS patterns of the celluloses. [Color figure can be viewed in the online issue, which is available at wileyonlinelibrary.com.]

min; then, the hydrolysis was stopped through the addition of 500 mL of water. The suspension was centrifuged at 10,000 rpm for 10 min and subsequently washed with water until a pH of about 7 was reached. The produced NCC I was dried at 90°C for 6 h.

Nanocellulose II (NCC II) Preparation

NCC II was obtained through the controlled hydrolysis of cellulose. An amount of 7 g of cellulose II was immersed in 70 mL of 64% H_2SO_4 and continuously stirred. Further steps were conducted as described for NCC I.

Composite Preparation

Chitosan/nanocellulose composites were produced by a solvent casting method. First, chitosan was dissolved in 2% CH_3COOH. Second, nanocelluloses at different concentrations were added to chitosan so that mixtures containing 5, 10, and 20% w/w NCC (in relation to the dry mass of chitosan) were obtained. The mixtures were stirred for 5 min at 3000 rpm, applied on Petri dishes, and left for 7 days at room temperature to evaporate the solvents.

Wide-Angle X-ray Scattering (WAXS)

The structures of the celluloses, nanocelluloses, and chitosan were analyzed by means of WAXS with Cu Kα radiation at 30 kV and a 25-mA anode excitation. The X-ray diffraction patterns were recorded for the angle range of from 5 to 30° with a step of 0.04°/3 s.

Determination of the Particle Size

The particle size distributions of cellulose I, cellulose II, NCC I, and NCC II were determined with a Zetasizer Nano ZS (Malvern Instruments, Ltd.); this enabled the measurement of the particle size in the range 0.6–6000 nm (noninvasive backscattering technique). The samples were dispersed in 2-propanol. The measurement involved the passing of a red laser beam with a wavelength of 663 nm through the material. During measurement, the intensity of fluctuations of scattered light was identified; these represented the illuminated particles of the sample. The particles within the fluid exhibited Brownian motion, and this made the measurement possible.

Determination of the Morphological Properties

The dispersion of NCC in the chitosan matrix and the particle sizes were observed with a scanning electron microscopy (SEM; Carl Zeiss AG–EVO 40 series) operated with an acceleration voltage of 18 kV. All the specimens were sputter-coated with gold before examination.

Fourier Transform Infrared (FTIR) Spectroscopy

The FTIR spectra of the celluloses and nanocelluloses were registered on an ATI Mattson InfinitySeries FTIR spectrometer equipped with a deuterated triglycine sulfate detector in the range from 500 to 4000 cm^{-1}.

Determination of the Tensile Properties

The tensile properties [YM, elongation at break (EB), and TS] of the composites were defined with a Zwick and Roell Allround-Line Z020 TEW testing machine. Samples 10 mm in width and about 0.1 mm in thickness were tested with a speed of 10 mm/min and an initial force of 0.2 N in accordance with ISO 527-3.

RESULTS AND DISCUSSION

Analysis of the Polymorphic Forms of the Celluloses and Nanocelluloses

The objective of the WAXS studies was to determine whether the mercerization caused full transformation from cellulose I into cellulose II. The supermolecular structures of the produced composites were tested as well. We observed that cellulose before mercerization exhibited three peaks at $2\theta = 15°$, 16°, 22.7° that are assigned to cellulose I (Figure 2). The cellulose that underwent alkali treatment showed peaks at 2θ values of 12, 20, and 22° that were characteristic for cellulose II. The WAXS pattern for cellulose II did not include any peaks from cellulose I; this proved that 100% of the starting cellulose was transformed into cellulose II. It was reported[15,23–25] that NaOH concentrations higher that 10% enable the transformation of the crystal structure of cellulose I into cellulose II. From a comparison of the WAXS patterns of the celluloses (Figure 2) and nanocelluloses (Figure 3), we concluded that NCC I consisted only of cellulose I and NCC II consisted entirely of cellulose II. The hydrolysis of cellulose enhanced the intensity of the characteristic peaks and also did not influence the crystallographic structure of NCC II; this was in accordance with the literature.[26]

FTIR spectra (Figure 4) were recorded to define and analyze the chemical structures of the produced cellulosic materials. According to the literature,[27] the spectra were characterized by the bands specified in Table I. All of the samples exhibited similar absorption bands; this confirmed that during chemical

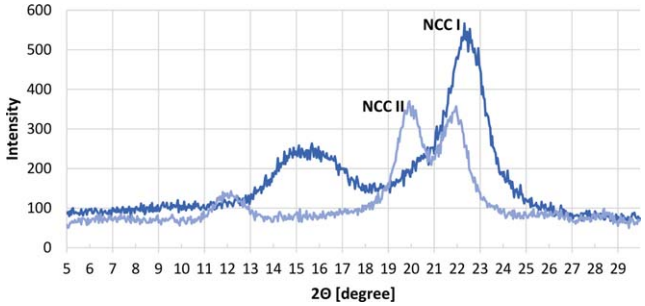

Figure 3. WAXS patterns of the nanocelluloses. [Color figure can be viewed in the online issue, which is available at wileyonlinelibrary.com.]

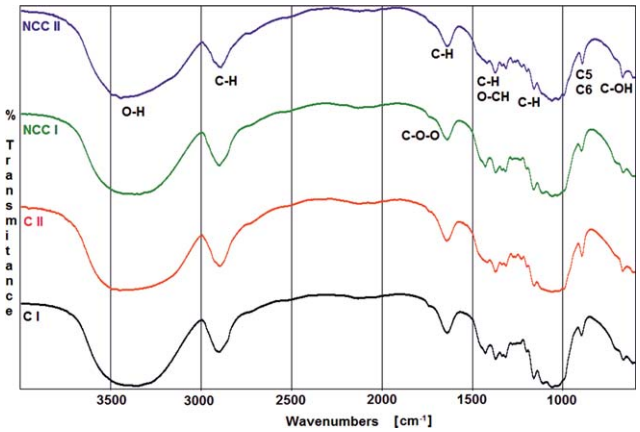

Figure 4. FTIR spectra of the celluloses and nanocelluloses (C I = cellulose I; C II = cellulose II). [Color figure can be viewed in the online issue, which is available at wileyonlinelibrary.com.]

treatment with 64% H_2SO_4 and 16% NaOH, no major harm was done to the chemical structure of cellulose. The band at about 1730 cm^{-1} may have been due to the C—O—O vibrations of the unconjugated carboxyl group of pectins, which were not removed during cellulose preparation.[28] However, the intensity of this peak was lower for cellulose II and NCC II than for cellulose I and NCC I; this indicated that the chemical treatment was effective. At 895 cm^{-1}, a band from the motions of the C5 and C6 atoms was observed. This band corresponded to cellulose II, and its intensity was used to measure the conversion from cellulose I to cellulose II.[15] This was also confirmed in our study because the intensities of the bands for cellulose II and NCC II were higher than those for cellulose I and NCC I.

Particle Size Distribution

The aim of the particle size distribution study was to confirm that a cellulose of nanometric size was produced and to define the influence of the crystallographic form of cellulose on its particle size. In Table II, the particle size distributions for the mercerized and nonmercerized cellulose are presented. The particle sizes of cellulose I were in the range from 106 to 5560 nm. It was also clear that the analyzed sample consisted of two main fractions that significantly differed in size. The biggest intensity had particles of a few micrometers. However, the particles with a size of 122 nm were characterized by a quite high intensity, 22.4%.

Table I. Vibrational Frequency Wave Numbers Attributed to the Celluloses and Nanocelluloses

Wave number (cm^{-1})	Vibrational assignment
~3344	O—H stretching
~2900	C—H bending
~1730	C—O—O
~1646	O—H stretching (moisture)
~1432	C—H and O—CH stretching (in-plane)
~1373	C—H bending
~895	Motions of the C5 and C6 atoms
~670	C—OH bending (out-of-plane)

Table II. Particle Size Distributions for Cellulose I and Cellulose II

Cellulose I		Cellulose II	
Intensity (%)	Diameter (nm)	Intensity (%)	Diameter (nm)
7.9	106	22.9	122
22.4	122	25.6	142
10.4	4150	1.1	164
26.6	4800	4.1	3580
32.7	5560	11.8	4150
		17.5	4800
		17	5560

For cellulose II, the intensity of the smaller particles was higher than for cellulose I, and particles 122 and 142 nm in size had the highest intensity. The second fraction consisted of particles with sizes between 3.58 and 5.56 μm. Therefore, we assumed that mercerization caused particle size reduction. However, the produced materials did not contain particles smaller than 100 nm, and therefore, they were not nanofillers by their traditional definition. For the products of the acid hydrolysis of cellulose I and cellulose II, the particle size distribution is shown in Table III. For both hydrolyzed celluloses, particles smaller than 100 nm were produced; this allowed us to call them nanocelluloses. NCC I consisted of particles with sizes in the range from 68.1 to 5560 nm, and even though the highest intensity was obtained for 5560-nm particles, the second most intense fraction had a size of 76.8 nm. NCC II particles had sizes between 78.8 and 1900 nm, and particles smaller than 100 nm were characterized by the highest intensities. Furthermore, the particle size dispersion was significantly smaller for NCC II compared to NCC I; this proved that in terms of particle sizes, the sample of NCC II was more homogeneous. On the basis of the presented data, we concluded that the acid hydrolysis that we performed was sufficient for producing nanometric

Table III. Particle Size Distributions for NCC I and NCC II

NCC I		NCC II	
Intensity (%)	Diameter (nm)	Intensity (%)	Diameter (nm)
5.7	68.1	33.3	78.8
20.7	76.8	19.2	91.3
9	91.3	10.6	1280
0.4	1480	21.3	1480
32.7	5560	14.9	1720
6.5	1720	0.7	1900
13.7	1990		
17	2300		
14.8	2670		
8.8	3090		
2.9	3580		

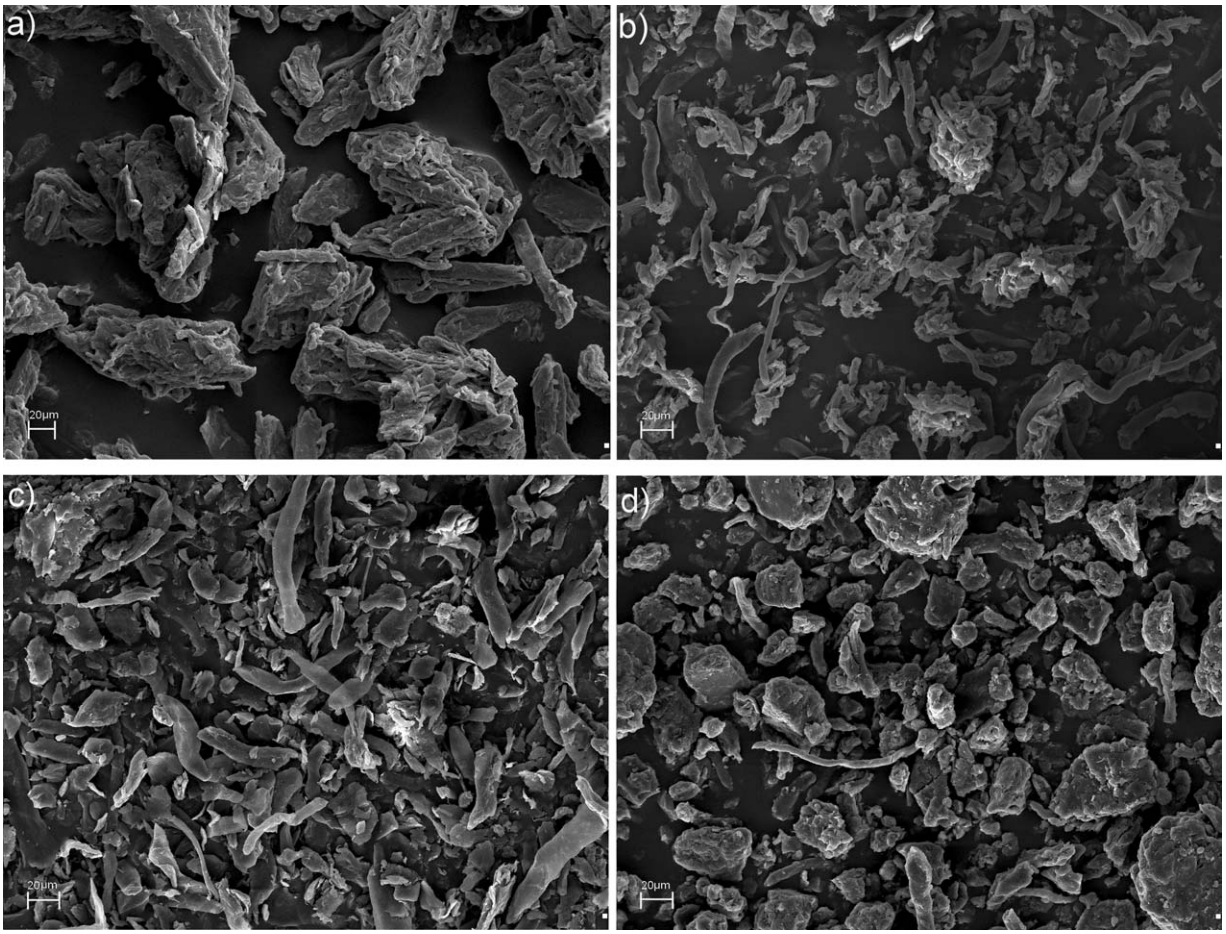

Figure 5. SEM microphotographs of the cellulose materials: (a) cellulose I, (b) cellulose II, (c) NCC I, and (d) NCC II (scale bar = 20 μm).

celluloses. Also, mercerization preceding the hydrolysis turned out to be effective in terms of decreasing the particle sizes.

However, what is a reason for cellulose II to be more prone to hydrolysis than cellulose I? First of all, the amorphous regions absorbed chemicals early, whereas the crystalline regions were less sensitive to chemical penetration.[29] Second, the internal surface area was reported to increase during the transformation from cellulose I to cellulose II.[30] Third, it is known that the parallel-chain arrangement of the cellulose I groups changed into a more stable antiparallel one in the cellulose II group.[31,32] That different crystallographic structure of cellulose II enabled a higher availability of cellulose structures; this was manifested in the smaller sizes of the particles. In our research, cellulose II turned out to be more susceptible to acid hydrolysis. The most probable reason for such a state of affairs was the increase in the internal surface and the change in the crystallographic structure; this included changes in the unit cell size and chain arrangement. Moreover, because cellulose II had fewer crystalline regions and was also more sensitive to hydrolysis than cellulose I, it seemed reasonable that we obtained more particles of NCC II than NCC I.[3,26] Even though small particles were obtained, some agglomeration was observed. The reason for this could have been hornification, the aggregation of cellulose taking place during its drying and caused by its high hydrophilic nature. This can be eliminated by the widely reported adjustment of the hydrophilic–hydrophobic balance and surface modeling.[33–41] It was also likely that during decantation after centrifugation, some nanoparticles were lost.

Morphology of the Samples

A comparison of the SEM microphotographs of cellulose I [Figure 5(a)] and cellulose II [Figure 5(b)] clearly confirmed the findings of particle size distribution. The particles of cellulose II were significantly smaller and less aggregated than those of cellulose I; this proved that mercerization influenced the morphology of the cellulosic materials. For nanocelluloses, more interesting than the particle size was the shape of the particles. NCC I [Figure 5(c)] had a fibrillar shape similar to cellulose, whereas NCC II [Figure 5(d)] tended to aggregate and form spherical or irregular particle shapes. Thus, mercerization and H_2SO_4 hydrolysis effectively diminished the size of the cellulose crystals.

Analysis of Composites

According to the literature, the supermolecular structure of chitosan is characterized by two peaks at 2θ values of about 12 and 19°;[42,43] in our studies, chitosan turned out to be amorphous (Figure 6). Two faint peaks were observed, although it was more likely to have been an effect of a temporary

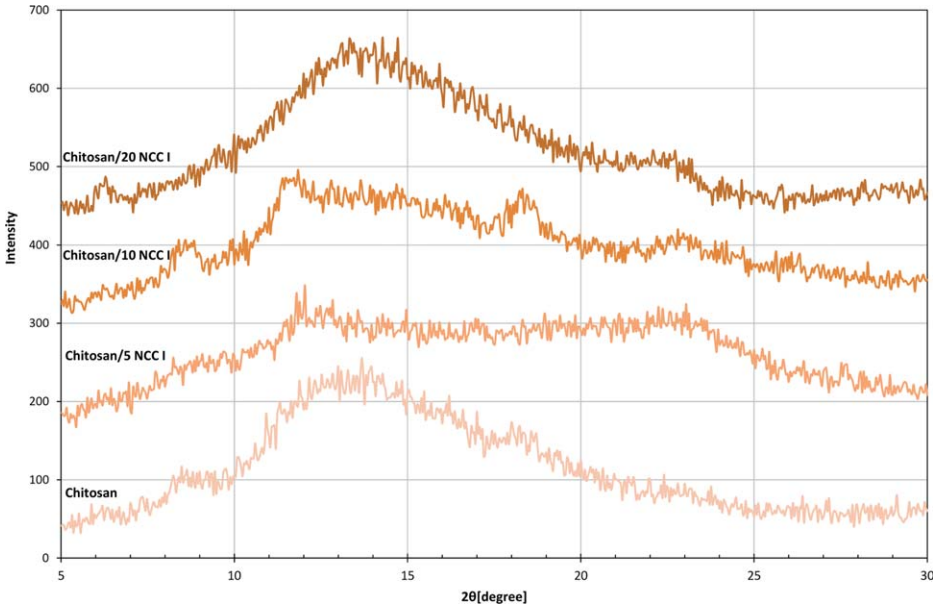

Figure 6. WAXS patterns of chitosan and its composites. [Color figure can be viewed in the online issue, which is available at wileyonlinelibrary.com.]

arrangement than one of the existence of a crystalline form. It was worth noticing, also on patterns recorded for the chitosan/NCC composites, that even for the composite with 20% NCC, no peaks indicating the crystalline structure were observed. Fernandes *et al.*[42] obtained similar results, where the peak at a 2θ of 22.7° was not registered until 60% nanofibrillated cellulose was added. Okano *et al.*[44] dissolved crystalline chitosan in aqueous acid, reprecipitated it in alkali, and freeze-dried it. The product was amorphous, with much improved reactivity; this was confirmed by the acetylation and enhanced adsorption capability. This indicated that in our composites, chitosan and NCC were chemically bonded, and the chitosan–nanocellulose interactions were stronger than those of nanocellulose–nanocellulose.

Table IV shows the effect of the nanofiller type and content on the mechanical properties of the nanocomposites, including TS, EB, and YM. It was worth noticing that in comparison with unmodified chitosan (YM = 236 MPa), all of the the nanocomposites showed enhancements in the YM parameter. YM reached a maximum value of 838 and 667 MPa for chitosan filled with 5% NCC I and 5% NCC II, respectively. With increasing nanofiller content up to 10%, YM of the nanocomposite films decreased, reaching minimum values that were still higher than that for neat chitosan. Similar findings were reported for TS. However, here, the difference between the nanocomposites containing 5% NCC I and 5% NCC II was more noticeable. TS for chitosan/5 NCC I reached a value of 29.2 MPa, whereas for chitosan/5 NCC II only 16 MPa; this, compared with that of chitosan (TS = 24.7 MPa), was a substantial decrease. Further addition of nanofiller impaired the tensile properties of the nanocomposites, although the discrepancy between films containing NCC I and NCC II was not as extensive. The increased YM suggested that formation of the composites with a uniform dispersion of NCC in the chitosan matrix was successful; this was also confirmed by the SEM microphotographs (Figure 7). We also observed that in terms of enhancing YM and TS, NCC I gave better results than NCC II but only for 5% nanofiller. For all of the other concentrations, values of both the YM and TS parameters were comparable; this proved that the polymorph form of the filler did not have significant influence on them.

In the case of larger contents of nanofiller, the influence of the polymorph form of cellulose on YM was not observed. The addition of 5% NCC was the most effective in terms of increasing both YM and TS. The fact that 5% NCC was optimum loading was also confirmed by Khan *et al.*[11] They claimed that the increase in TS of the NCC-loaded chitosan composites was due to (1) the reinforcing effect at the nanocrystal–chitosan interface caused by effective stress transfer and (2) nanocrystal–polymer interactions. As already proven by Okano *et al.*,[44] the amorphous chitosan was highly reactive; thus, it was very likely that the cationic amine groups of chitosan were bonded with the anionic sulfate groups of NCC. This resulted in improved tensile properties. As expected, in our research, the addition of NCC had a great impact on the EB values. With the addition of nanofiller, EB dropped from 41.9% for unmodified chitosan to 23.4 and 10.4% for chitosan/5 NCC I and chitosan/5 NCC II, respectively. For 10 and 20% loading values of this parameter, the EB values dropped and were in the range from 2.3 to 3%. This sharp decrease in the EB value indicated that motion of the chitosan matrix was restricted because of its interactions with NCC; this was consistent with other publications.[45] The decrease of the EB parameter with increasing nanofiller content is a well-known phenomenon. Hosseini *et al.*[46] prepared bionanocomposite films consisting of a fish gelatin matrix and chitosan nanoparticles. They reported that with an increase in the nanofiller content, the EB parameter of the nanocomposites decreased from 102.04% for the pure matrix to 32.73% for the film loaded with 8% nanochitosan. Similar results were observed by Dai *et al.*,[47] who used taro starch nanoparticles as

Table IV. Mechanical Properties of the Chitosan/NCC Composites (Average Value ± Standard Deviation)

	YM (MPa)	TS (MPa)	EB (%)
Chitosan	236 ± 56	24.7 ± 1.5	41.9 ± 4.8
Chitosan/5 NCC I	838 ± 55	29.2 ± 1.0	23.4 ± 2.5
Chitosan/10 NCC I	273 ± 33	13.4 ± 0.6	3.4 ± 0.3
Chitosan/20 NCC I	359 ±59	11.5 ± 1.2	2.3 ± 1.4
Chitosan/5 NCC II	667± 58	16.0 ± 1.1	10.4 ± 1.4
Chitosan/10 NCC II	284 ± 36	13.1 ± 1.1	3.0 ± 0.5
Chitosan/20 NCC II	342 ± 35	15.7 ± 1.0	3.0 ± 0.1

reinforcing agents in corn starch. They found that the EB of the nanocomposites decreased as the nanoparticle content increased (EB ≈ 84 and 58% for 0 and 15% contents of nanofiller, respectively). This brittleness of films caused by intermolecular forces is a very common issue among biopolymers and can be overcome by the addition of a plasticizer. Azaredo *et al.*[8] attempted to plasticize chitosan/nanocellulose fibers films with glycerol. The addition of 30% w/w glycerol increased EB up to 34.6%; this was still a poor value in comparison with those of some synthetic polymers but a relatively high one in comparison with that of the control sample (EB = 7.9%).

Mechanical testing suggested that the tensile properties of the composites were closely related to the polymorphic variety of cellulose. The results show that the composites containing the filler based on cellulose II were characterized by reduced mechanical parameters. Similar results were presented by Marcovich *et al.*,[48] who found that the alkalization reaction of wood decreased the mechanical properties of the composites. However, some authors, such as Pimenta *et al.*,[49] Ichazo *et al.*,[50] and Borysiak,[51] also confirmed the positive role of mercerization in the improvement of the macroscopic properties of the composites.

The discussion of the results presented in this section prove that the modification of cellulose by alkali had an important influence on the mechanical properties. SEM microphotographs provided an explanation for this interesting observation. As already discussed, the surfaces of both types of NCC [Figure 5(c,d)] differed significantly. The shape of the filler was associated with an important parameter: the aspect ratio. This is defined as the ratio of the length to the width of the filler, and it determines both the anisotropic phase formation and the reinforcing properties.[52] A relatively large aspect ratio is responsible for high reinforcing properties and, therefore, has been studied extensively in the literature. In our research, a greater reinforcing effect was obtained for composites of NCC I with high aspect ratios.

The SEM microphotographs of the nanocomposites based on NCC I and NCC II (Figure 7) showed that both types of nanocomposites were characterized by a good distribution of nanoparticles in the chitosan matrix. After the films were dried, a change in the dimensions of the nanofillers was observed. The size of the nanofiller in the films was significantly smaller than that for the cellulose powders. This could have been a result of solvent–nanofiller interactions during the production of films. This coincided with the results obtained from the WAXS studies and, therefore, proved that strong interactions between nanocellulose and chitosan were obtained.

To the best of our knowledge, this is the first publication covering crystallographic forms of nanocellulose and its influence on the properties of nanocellulose-based composites; this constitutes its scientific novelty. Numerous methods were applied to fully characterize the produced materials, and some of the results confirmed data collected by other researches. At present,

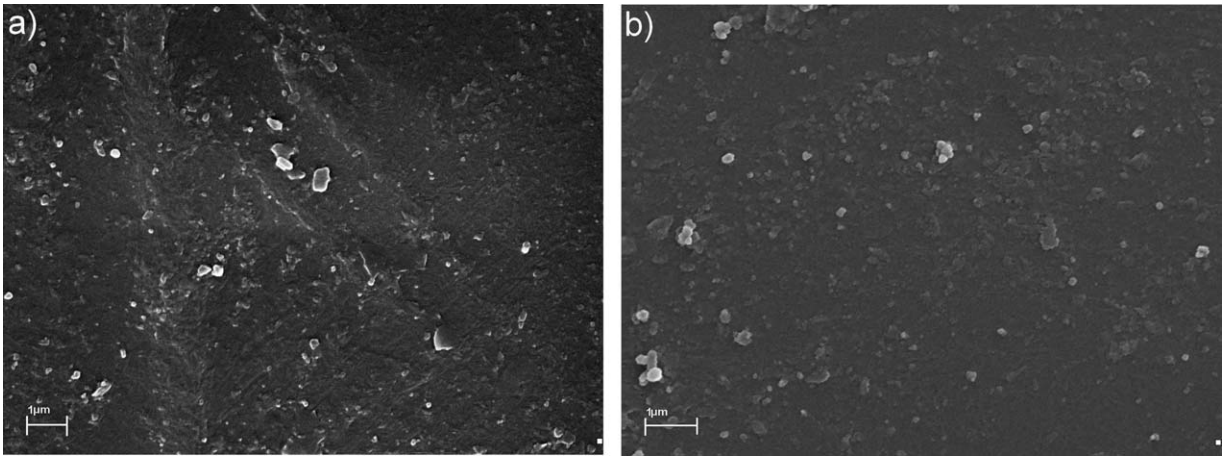

Figure 7. SEM micrographs of the nanocellulose composites: (a) chitosan/20 NCC I and (b) chitosan/20 NCC II (scale bar = 1 µm).

we are developing an innovative method for the production of nanocellulose and are modifying the final mechanical properties of the composites.

CONCLUSIONS

Cellulose and nanocellulose powders and chitosan/nanocellulose composites were investigated in terms of their morphologies and tensile properties. Mercerization preceding hydrolysis turned out to be an effective method for producing nanometric particles. NCC I had particle sizes ranging from 68.1 to 5560 nm, whereas NCC II particles had sizes between 78.8 and 1900 nm. The presence of nanometric cellulose particles was not the only factor determining the improvement of the mechanical properties of the chitosan/nanocellulose composites. It was interesting that better mechanical properties were obtained for the chitosan/5% NCC I nanocomposites, even though the fraction of nanometric NCC II was higher compared to that of NCC I. For the remaining concentrations, the mechanical properties of the composites were comparable. This allows us to state that the polymorph form of the filler did have any major influence on the mechanical properties of the composites. The addition of 5% NCC I to chitosan was the most effective in terms of increasing TM and TS. These studies show that the shape of the nanofiller determined by its aspect ratio was an extremely important parameter, and it had to be taken into consideration during the interpretation of the results.

ACKNOWLEDGMENTS

This research was supported by the Poznan University of Technology (contract grant sponsor 03/32/DSPB/0503).

REFERENCES

1. Rao, S. S.; Prasad, S.; Sharma, R. S. Presented at the International Conference on Recent Developments in Structural Engineering (RDSE-2007), Manipal, India, Aug–Sept **2007**
2. Pilla, S. In Handbook of Bioplastics and Biocomposites Engineering Applications; Pilla, S., Ed.; Wiley: New York, **2011**; Chapter 1, p 1.
3. Wertz, J.; Bédué, O.; Mercier, J. P. In Cellulose Science and Technology; EPFL: Lausanne, Switzerland, **2010**; Chapter 1, p 21, Chapter 3, p 101.
4. Moon, R. J.; Martini, A.; Nairn, J.; Simonsenf, J.; Youngblood, J. *Chem. Soc. Rev.* **2011**, *40*, 3941.
5. Klemm, D.; Kramer, F.; Moritz, S.; Lindström, T.; Ankerfors, M.; Gray, D.; Dorris, A. *Angew. Chem. Int. Ed.* **2011**, *50*, 5438.
6. Habibi, Y. In Biopolymer Nanocomposites Processing, Properties, and Applications; Dufresne, A., Thomas, S., Pothan, L. A., Grossman, R. F., Nwabunma, D., Eds.; Wiley: New York, **2013**; Chapter 16, p 367.
7. Suyatma, N. E.; Tighzert, L.; Copinet, A. *J. Agric. Food. Chem.* **2005**, *53*, 3950.
8. Azeredo, H. M.; Mattoso, L. H.; Avena-Bustillos, R. J.; Filho, G. C.; Munford, M. L.; Wood, D.; McHugh, T. H. *J. Food Sci.* **2010**, *75*, N1.
9. Nordqvist, D.; Idermark, J.; Hedenqvist, M.; Gällstedt, M.; Ankerfors, M.; Lindström, T. *Biomacromolecules* **2007**, *8*, 2398.
10. Kim, Y.; Jung, R.; Kim, H. S.; Jin, H. J. *Curr. Appl. Phys.* **2009**, *9*, S69.
11. Khan, A.; Khan, R. A.; Salmieri, S.; Le Tien, C.; Riedl, B.; Bouchard, J.; Chauve, G.; Tan, V.; Kamal, M. R.; Lacroix, M. *Carbohydr. Polym.* **2012**, *90*, 1601.
12. Dehnada, D.; Emam-Djomehb, Z.; Mirzaeia, H.; Jafaria, S. M.; Dadashi, S. *Carbohydr. Polym.* **2014**, *105*, 222.
13. Dehnad, D.; Mirzaeia, H.; Emam-Djomehb, Z.; Jafaria, S. M.; Dadashi, S. *Carbohydr. Polym.* **2014**, *109*, 148.
14. Velásquez-Cock, J.; Ramírez, E.; Betancourt, S.; Putaux, J.-L.; Osorio, M.; Castro, C.; Gañán, P.; Zuluaga, R. *Int. J. Biol. Macromol.* **2014**, *69*, 208.
15. Dinand, E.; Vignon, M.; Chanzy, H.; Heux, L. *Cellulose* **2002**, *9*, 7.
16. Yue, Y.; Zhou, C.; French, A. D.; Xia, G.; Han, G.; Wang, Q.; Wu, Q. *Cellulose* **2012**, *19*, 1173.
17. Nishiyama, Y.; Johnson, G. P.; French, A. D.; Forsyth, V. T.; Langan, P. *Biomacromolecules* **2008**, *9*, 3133.
18. Langan, P.; Nishiyama, Y.; Chanzy, H. *J. Am. Chem. Soc.* **1999**, *121*, 9940.
19. Amash, A.; Zugenmaier, P. *Polymer* **2000**, *41*, 1589.
20. Zafeiropoulos, N. E.; Baillie, C. A.; Matthews, F. L. *Compos. A* **2001**, *32*, 525.
21. Borysiak, S. *J. Therm. Anal. Calorim.* **2012**, *109*, 595.
22. Quillin, D. T.; Caulfield, D. F.; Koutzky, J. A. *J. Appl. Polym. Sci.* **1993**, *50*, 1187.
23. Gwon, J. G.; Lee, S. Y.; Chun, S. J.; Doh, G. H.; Kim, J. H. *Korean J. Chem. Eng.* **2010**, *27*, 651.
24. Borysiak, S.; Garbarczyk, J. *Fibres Text. East. Eur.* **2003**, *11*, 104.
25. Zugenmaier, P. *Prog. Polym. Sci.* **2001**, *26*, 1341.
26. Cao, Y.; Tan, H. *Enzyme Microb. Technol.* **2005**, *36*, 314.
27. Satyamurthy, P.; Vigneshwaran, N. *Enzyme Microb. Technol.* **2013**, *52*, 20.
28. Dymińska, L.; Gągor, A.; Hanuza, J.; Kulma, A.; Preisner, M.; Żuk, M.; Szatkowski, M.; Szopa, J. *J. Mol. Struct.* **2014**, *1074*, 321.
29. Mwaikambo, L. Y.; Ansell, M. P. *J. Appl. Polym. Sci.* **2002**, *84*, 2222.
30. Ishikawa, A.; Okano, T. *Polymer* **1997**, *38*, 463.
31. Okano, T.; Sarko, A. *J. Appl. Polym. Sci.* **1985**, *30*, 325.
32. Sao, K. P.; Samantaray, B. K.; Bhattacherjee, S. *J. Appl. Polym. Sci.* **1996**, *60*, 919.
33. Habibi, Y. *Chem. Soc. Rev.* **2014**, *43*, 1519.
34. Islam, M. T.; Alam, M. M.; Zoccola, M. *Int. J. Innov. Res. Sci. Eng. Technol.* **2013**, *2*, 5444.
35. Braun, B.; Dorgan, J. R. *Biomacromolecules* **2009**, *10*, 334.
36. Ho, T. T. T.; Zimmermann, T.; Hauert, R.; Caseri, W. *Cellulose* **2011**, *18*, 1391.

37. Kalia, S.; Dufresne, A.; Cherian, B. M.; Kaith, B. S.; Avérous, L.; Njuguna, J.; Nassiopoulos, E. *Int. J. Polym. Sci.* **2011**, Vol. 2011, 1.

38. Dufresne, A. In Nanocellulose from Nature to High Performance Tailored Materials; de Gruyter: Berlin, **2012**; Chapter 5, p 147.

39. Siqueira, G.; Bras, J.; Dufresne, A. *Langmuir* **2010**, *26*, 402.

40. Cherian, B. M.; Leao, A. L.; Ferreira de Souza, S.; Thomas, S.; Pothan, L. A.; Kottaisamy, M. In Cellulose Fibers: Bio- and Nano-Polymer Composites: Green Chemistry and Technology; Kalia, S., Kaith, B. S., Kaur, I., Eds.; Springer: Berlin, **2011**; Chapter 21, p 539.

41. Habibi, Y.; Lucia, L. A.; Rojas, O. J. *Chem. Rev.* **2010**, *110*, 3479.

42. Fernandes, S. C. M.; Freire, C. S. R.; Silvestres, A. J. D.; Neto, C. P.; Gandini, A.; Berglund, L. A.; Salmén, L. *Carbohydr. Polym.* **2010**, *81*, 394.

43. Zong, Z.; Kimura, Y.; Takahashi, M.; Yamane, H. *Polymer* **2000**, *41*, 899.

44. Okano, K.; Minagawa, T.; Yang, J.; Shimojoh, M.; Kurita, K. *Polym. Bull.* **2009**, *62*, 119.

45. Azizi Samir, M. A. S.; Alloin, F.; Sanchez, J. Y.; Dufresne, A. *Polymer* **2004**, *45*, 4149.

46. Hosseini, S. F.; Razaei, M.; Zandi, M.; Farahmandghavi, F. *Food Hydrocolloids* **2015**, *44*, 172.

47. Dai, L.; Qiu, C.; Xiong, L.; Sun, Q. *Food Chem.* **2015**, *174*, 82.

48. Marcovich, N. E.; Aranguren, M. I.; Reboredo, M. M. *Polymer* **2001**, *42*, 815.

49. Pimenta, M. T. B.; Carvalho, A. J. F.; Vilaseca, F.; Gironès, J.; Lopez, J. P.; Mutjé, P.; Curvelo, A. A. S. *J. Polym. Environ.* **2008**, *16*, 35.

50. Ichazo, M. N.; Albano, C.; Gonzalez, J.; Perera, R.; Candal, M. V. *Compos. Struct.* **2001**, *54*, 207.

51. Borysiak, S. *J. Appl. Polym. Sci.* **2012**, *127*, 1309.

52. Boufi, S.; Kaddami, H.; Dufresne, A. *Macromol. Mater. Eng.* **2014**, *299*, 560.